ELSEVIER

Ceramics International 33 (2007) 439–445

CERAMICS INTERNATIONAL

www.elsevier.com/locate/ceramint

Preparation and friction behavior of carbon fiber reinforced silicon carbide matrix composites

Yongdong Xu *, Yani Zhang, Laifei Cheng, Litong Zhang, Jianjun Lou, Junzhan Zhang

National Key Laboratory of Thermostructure Composite Materials, P.O. Box 547, Northwestern Polytechnical University, Xi'an, Shaanxi 710072, China

Received 22 August 2005; received in revised form 2 September 2005; accepted 25 October 2005
Available online 28 February 2006

Abstract

Carbon fiber reinforced silicon carbide matrix composites have received considerable attention because of their superior friction behavior. In this paper, carbon/silicon carbide composites were fabricated by chemical vapor infiltration. The microstructure, mechanical properties, and the friction behavior were investigated. The carbon fiber preform was fabricated with the three dimension needling method, and the infiltrated carbon/silicon carbide (C/SiC) composites exhibited excellent shear strength. The in-plane shear strength and the inter-laminar shear strength are 85 and 27 MPa, respectively. The composites show non-brittle failure behavior resulting from fiber pull-out as well as fiber cluster pull-out. The friction behavior and friction stability are significantly improved by increasing both the density and carbon content of the composites. If the density of the composite is 2.3 g cm^{-3}, the coefficient of friction measured is 0.23, the coefficient of friction stability (as it will be defined later on) is 0.43, and the liner wear rate is less than 9.3 μm/cycle. Moreover, the C/SiC composites demonstrate a good friction property against fading versus several braking stops. The rapid increase of friction coefficient approaching the end of braking is mainly related to the increasing of surface temperature in a short time and the enhanced adhesion and abrasion of contact conjunctions and asperities. The friction surface is covered with wear debris including flake materials and fragments of carbon fiber. The micro-cracks and grooves observed on the friction surface are significantly determined by cyclic mechanical and thermal stresses.

Keywords: Carbon/silicon carbide composites; Chemical vapor infiltration; Friction behavior

1. Introduction

The most common friction materials presently used in aircraft brakes are carbon composites and metallic friction pads or rings. However, the disadvantages of steel brakes such as the high weight and the poor performance at high temperature are key issues that limit their application [1]. The introduction of carbon composites fulfills a significant reduction of weight, high performance and long lifetime. However, carbon/carbon (C/C) brakes suffer from their insufficient stability of coefficient of friction caused by humidity and temperature, high cost, and large stack volume. Further more, in oxidative condition the fiber and matrix in carbon composites degrade above 450 °C and service life is limited, which could potentially lead to brake failure and prevented their use as brake materials in passenger cars and trains or emergency brakes of lifts and cranes [2–4]. The non-oxide ceramic composites, such as carbon fiber reinforced silicon carbide (C/SiC) composites, in comparison to C/C composites, show considerably lower open porosity (less than 5%), a moderately higher density (about 2 g/cm^3), smaller stack volume as brake disks, lower sensibility to surroundings and oxidation, and higher service temperature as lightweight structure materials in aerospace technology which is limited to about 1000 °C. The silicon carbide matrix offers very good oxidation and thermal shock resistance and a good compatibility with carbon fibers [5–7]. Additionally, the limited friction data indicates that this material has the potential to offer stable coefficient of frictions [8]. Presently, an increasing attention is being paid to these C/SiC composites that could overcome the shortcoming of carbon composites without sacrificing their advantages as brake disks.

As brake disks are the key parts in tribo-system for the takeoff and landing of aircraft, the C/SiC composites could

* Corresponding author. Tel.: +86 29 88494619; fax: +86 29 88494620.
E-mail address: ydxu@nwpu.edu.cn (Y. Xu).

0272-8842/$32.00
doi:10.1016/j.ceramint.2005.10.008

overcome the tribological shortcoming of traditional friction materials at high temperature, which suggested a promising future of the C/SiC ceramic composites as aircraft brakes. Several institutes and industries now exist to investigate CMC materials for their use as frictional materials for brake pads and disks. In 2000, the C/SiC brakes were introduced in a special edition of the Mercedes S class coupe and Porsche 911 Turbo [7]. Recently, four companies in the USA (Aircraft braking systems, Goodrich, Honeywell and Parker-Hannifin) formed a Ceramic Composite Aircraft Brake (CCAB) Consortium to study ceramic materials for aircraft brake application [9].

Based on the C/SiC ceramic matrix composites prepared by chemical vapor infiltration, the objective of the present work is to study the microstructure and mechanical properties of the 3D needling composite materials, and to investigate the braking behavior and wear of the C/SiC composites.

2. Experimental procedures

2.1. C/SiC composites preparation

The C/SiC composites were prepared by chemical vapor infiltration (CVI) method, which was mainly achieved in two steps. Step I: the carbon fiber (T300, 3 K) preform was prepared by the three-dimensional needling method, starting with the repeated overlapping of 0° non-woven cloth layer, short-cut web layer, and 90° non-woven cloth layer. The needling method was then applied to joint different lamina by introducing carbon fiber bundles perpendicular to the lamina direction. Then the preform was infiltrated with pyrolytic carbon (PyC), the thickness was about 200 nm, which resulted in the carbon/carbon composites. Four types of specimens namely A–D were made in this carbon/carbon intermediate stage. Step II: carbon fiber reinforced silicon carbide matrix composites were prepared by chemical vapor infiltration of SiC with carbon preform. The final three-dimensional C/SiC composite is shown in Fig. 1. The specimens of type A were directly infiltrated with silicon carbide (SiC) matrix. Methyltrichlorosilane (MTS, CH_3 $SiCl_3$) was used for the deposition of the SiC matrix. MTS vapor was carried by bubbling hydrogen. The specimens of types B–D were pretreated with graphitization, and then infiltrated with SiC by chemical vapor infiltration. The temperature was 1000 °C during the CVI process, and the temperature of graphitization treatment was 1800 °C for 2 h. The density, C-content and the SiC-content of the C/SiC composite specimens are listed in Table 1.

2.2. Braking tests of C/SiC composites

The braking performance of C/SiC composites were measured under atmosphere condition in the disk-on-disk configuration, which simulated the normal landing of the

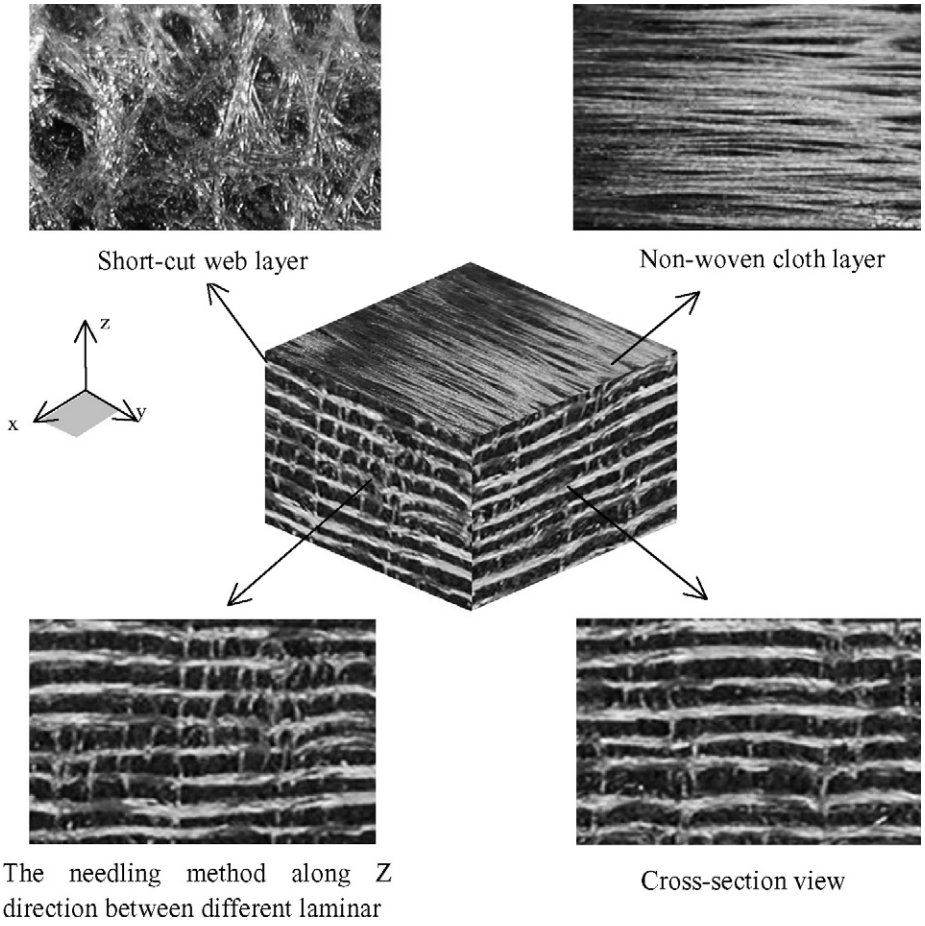

Fig. 1. Three-dimensional view of the 3D C/SiC composites' microstructure.

Table 1
The mechanical properties of the 3D C/SiC composites

Mechanical property	Unit	Results at r.t.
Density	g/cm^3	Type A: 1.6; Type B: 1.8; Type C: 2.2; Type D 2.3
C-content	wt.%	Type A: 35; Type B: 45; Type C: 50; Type D: 65
SiC-content	wt.%	Type A: 65; Type B: 55; Type C: 50; Type D: 35
Tensile strength[a]	MPa	126
Flexural strength[a]	MPa	287
Compression strength[a]	MPa	154
In-plane shear strength[a]	MPa	85
Inter-laminar shear strength[a]	MPa	27

[a] The strengths in Table 1 were tested for the sample of Type D.

aircraft by the surface contacting of a pair of brake disks. In the braking tests, one disk simulates the rotating disk of the tribo-system, and the other simulates the stationary disk. The given rotating velocity and the contact pressure were 8000 r/min and 0.82 MPa, respectively. The parameters (rotating velocity n (r/min), liner wear rate on one side of disk in each braking cycle l (μm/cycle), braking torque M_{cp} (Nm), surface temperature T (°C) and braking time t (s)) were continuously recorded during braking tests. The coefficient of friction stability S which represents the fluctuation of COF during braking test can be described as:

$$S = \frac{\mu_{cp}}{\mu_{max}} \quad (1)$$

where μ_{cp} is the average coefficient of friction, and μ_{max} is the maximum coefficient of friction.

2.3. Measurement of density and observation of surface microstructure

The densities of C/SiC composite samples were measured by Archimedes' method. The microstructure was investigated by an optic microscope and the SEM (S-4700) analysis.

2.4. Measurement of mechanical properties

Mechanical properties of the 3D C/SiC composites were investigated under tensile, compressive, bending and shear loading. The samples for measurement were cut from the original C/SiC bulk materials. The sample size were 120 mm × 18 mm × 3.5 mm for tension test, 20 mm × 10 mm × 10 mm for compressive test, 40 mm × 4 mm × 3 mm for bending test, and 30 mm × 25 mm × 3.5 mm for inter-laminar shear test. All the measurements of mechanical properties were performed on an Instron 1196 test machine, with a loading velocity of 0.005 mm/min.

3. Results and discussion

3.1. Mechanical properties of the C/SiC composites

Mechanical properties of the 3D C/SiC composites were investigated under tensile, compact, bending and shear loading. The corresponding strength data of C/SiC composites are listed in Table 1, and the microstructural observation of different failure behavior is shown in Fig. 2. The variation of failure behavior of composites was caused by alteration of the interfacial bonding between fiber and matrix [10]. The tensile stress within interfacial phase along the fiber radial direction was generated after the composites cooled down from the infiltration temperature to room temperature. Thereby, it was easy for the carbon fiber to debond and be pulled out from the silicon carbide matrix. The in-plane shear strength and the inter-laminar shear strength were tested along the loading directions as the arrows marked in Fig. 2(c and d).

The fibers that be pulled out from the matrix after damage under tensile and bending load still connected the materials, resulted in the non-brittle failure behavior of the composites and avoided the brittle failure mode (Fig. 2(a and b)). The tensile strength and flexural strength of C/SiC composites were 126 and 287 MPa, respectively. The mis-match along the fiber axis of thermal expansion coefficients (TECs) between the silicon carbide matrix and the fiber resulted in many micro-cracks in the matrix. These micro-cracks had some contribution to the non-brittle failure behavior by deflection of the main cracks (Fig. 2(a)). Under compressive load, as the dispersing and the carrying capacity losing of fiber bundles caused by interfacial debonding, the delamination and non-woven fiber extrusion occurred in materials. The compression strength was 154 MPa. The introduction of fiber bundles which perpendicular to the laminar direction effectively improved the shear resistance of C/SiC materials because of the preventing of cracks expansion. The in-plane shear strength and the inter-laminar shear strength of the C/SiC composites were 85 and 27 MPa, respectively. As Fig. 2(c) shows, the micro-crack was found where the diagonal split occurred in the damaged in-plane shear specimen. Fig. 2(d) shows the damaged inter-laminar shear specimen. When observed by the SEM analysis, the micrograph of the fracture surface of inter-laminar shear specimen showed fracture and pull out of carbon fibers (Fig. 2(e)). It is concluded that the C/SiC composites with three-dimensional needling method exhibit excellent shear strength, as it could be expected.

3.2. Braking behavior of the C/SiC for different specimens

The braking behaviour of C/SiC composites was characterized with the parameters of surface temperature, coefficient of

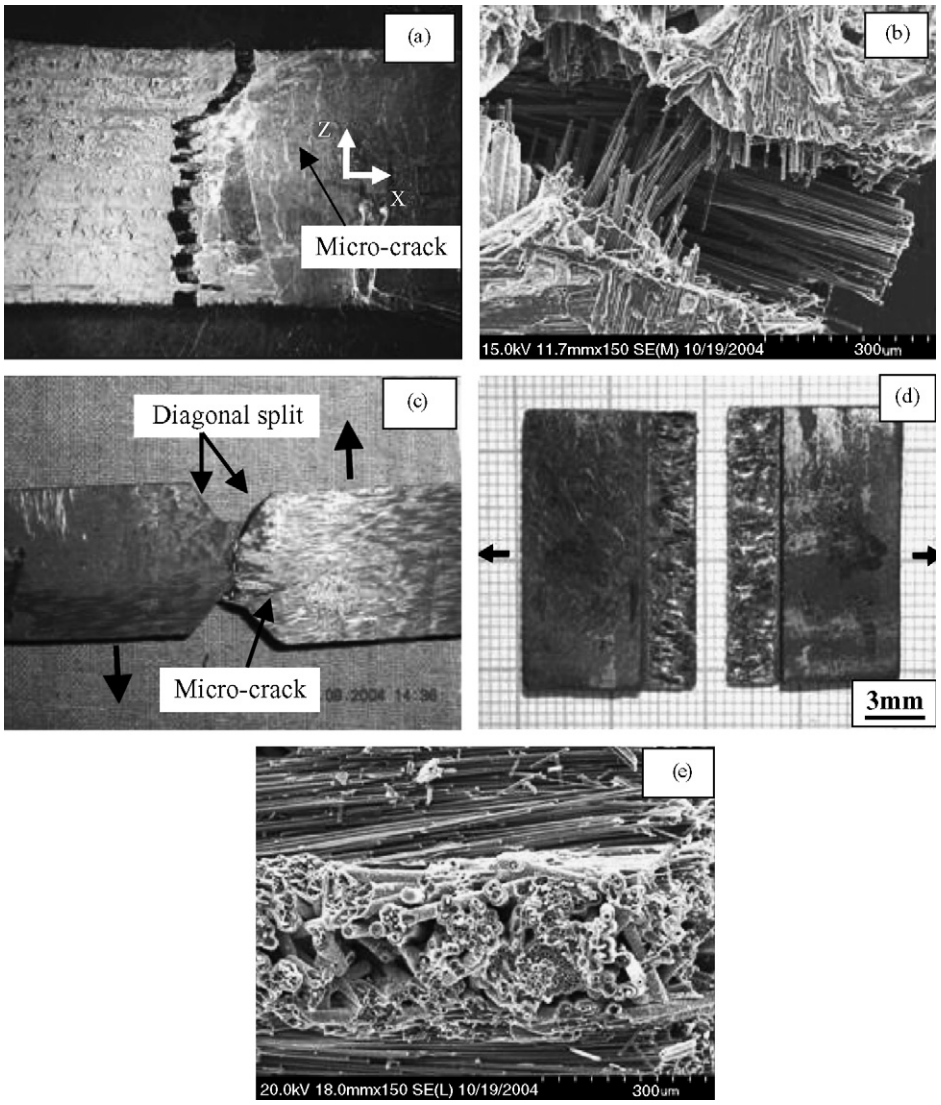

Fig. 2. Optical macrographs and SEM micrograph of damaged specimen; (a) damaged tensile specimen; (b) damaged bending specimen; (c) damaged in-plane shear specimen; (c) damaged inter-laminar shear specimen and (e) fracture surface of inter-laminar shear specimen.

friction, friction torque and sliding velocity as shown in Fig. 3. The coefficient of friction (COF) was observed to be proportional to the friction torque (curves 3 and 4 in Fig. 3) a fact related to the given constant applied pressure. The coefficient of friction curve could be divided into three parts, a narrow peak at the start of braking, a relative smooth middle stage, and a rapid increasing stage when approaching the end. The COF in the beginning of braking was mainly affected by the coverage of surfaces by absorbed water molecules during the cooling in the air after each braking stop. In the middle stage COF was determined by the solid–solid contact of asperities on surfaces of disks resulting in an adhesion force F_{ad}. The value of COF was established from the product of shear strength τ_s of adhesion junction or asperities and the true area of solid contact A_s. When approaching the end of braking, the sliding velocity decreased and the surface temperature increased to about 500 °C in a short time, which enhanced the adhesion and abrasion of the contact conjunctions and asperities, produced higher mechanical deformation resistance and sliding resistance (higher friction force). Thereby, a rapid increasing of COF value was caused when approaching the end of braking.

The coefficient of friction (COF) for the four types C/SiC disks during the braking tests are comparatively investigated in Fig. 4. The average value of COF elevates, the first peak value decreases, and the braking time (distance between start point

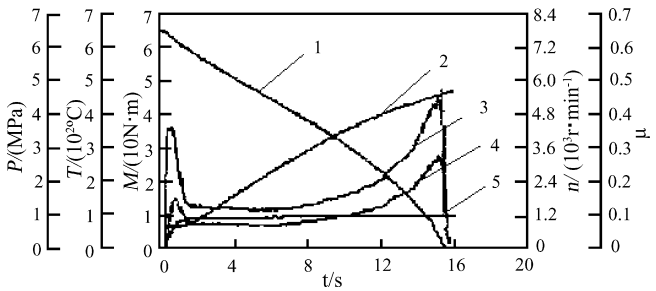

Fig. 3. The curves of friction parameters of C/SiC disks. (1) Sliding velocity, (2) surface temperature, (3) coefficient of friction, (4) friction torque and (5) surface pressure.

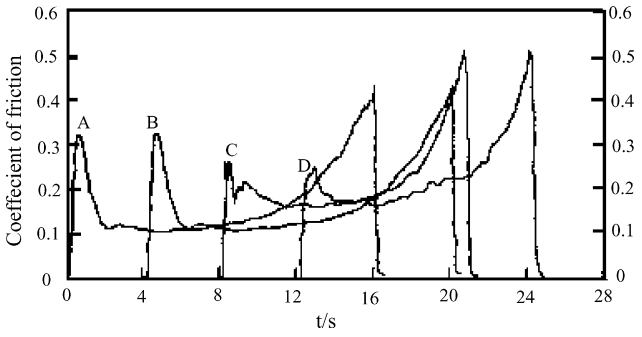

Fig. 4. The friction coefficient curves of C/SiC disks of different types.

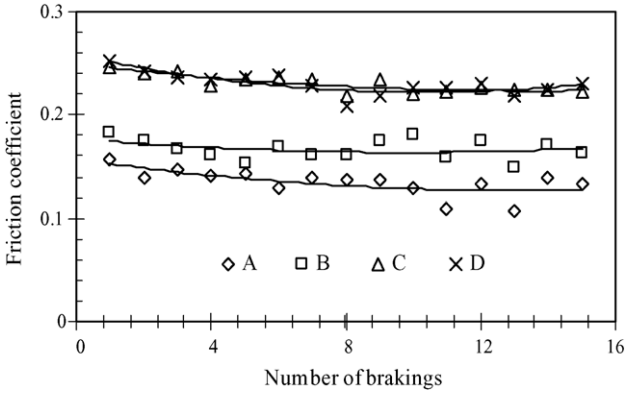

Fig. 5. The relationship of friction coefficients and braking number of C/SiC disks.

and end point for each curve) shortens with the increase of carbon content and density from types A to D. Generally, within the same roughness the higher the hardness is, the lower the COF. Under the same machining condition, the four types C/SiC disks show different COF value because of their different hardness. The hardness of types B–D is lower than that of type A because of the graphitization treatment (HTT) and the higher carbon content, therefore, the composite with lower hardness exhibits the higher COF values. It can be concluded that the COF increases with the increase of carbon content in C/SiC composites.

Considering the cyclic using and the friction stability of C/SiC composites disks, the influence of braking number on the coefficient of friction (COF) was analyzed. Fig. 5 shows that the COF value decreases with a small range of about 0.01–0.02 versus the braking number, which suggests a good stability of braking against fading versus several braking stops. Similarly, the COF value for each braking cycle shows elevated trend from types A to D as Fig. 4 indicated above. Moreover, the fluctuation range of COF value is obviously reduced from types A to D for several braking stops, which suggests a promising improvement of friction stability by increasing carbon content and density of C/SiC composites.

3.3. Wear and microstructure on surfaces of the C/SiC composites

The coefficient of friction (COF) is determined by several factors, which include the mechanical deformation of the contact junction or asperities, the groove effect of wear debris, the adhesion and abrasion between the contact surfaces [11]. The fluctuation of COF is related with the roughness, hardness, temperature, sliding velocity and wear mechanisms on friction surfaces.

The wear-induced surfaces were significantly determined by the abrasion and damage mechanism between the contact surfaces, which resulted in the variation of the COF value. The surface quality of C/SiC disks were observed by an optic microscope after the braking tests (Figs. 6 and 7). The disk surfaces of types B–D present similar wear state after braking, which derived from the graphitization pre-treatment and the higher carbon content than that of type A. As shown in Fig. 6(a), the real contact area (effective friction area) approaches the nominal area, and the wideness of outside-annulus and inside-annulus on the surface is nearly zero. However, the disk surface of type A (Fig. 6(b)) presents the non-brittle luster. The effective friction area of type A is much smaller than that of types B–D, specially, several concentric rings are distributed on the surface. The form of the friction rings (Fig. 7(a)) is derived from the relative sliding of hard-phase material with higher SiC contend of type A than that of types B–D on friction surfaces.

The wear rate of the C/SiC composites were characterized in terms of the linear wear rate on one side of disk in one braking cycle. As listed in Table 2, the linear wear rate of the rotating disks in each type is much higher than that of the stationary disks. The average linear wear rate of the two disks in four types is less than 9.3 μm/cycle. The linear wear rate was observed to

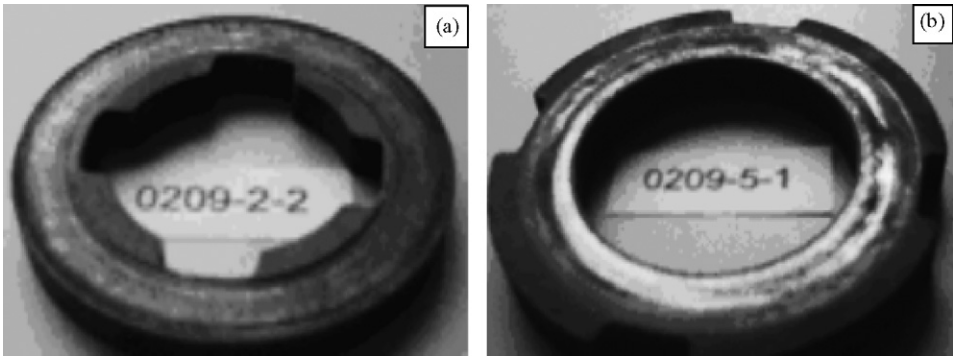

Fig. 6. The friction surfaces of C/SiC disks.

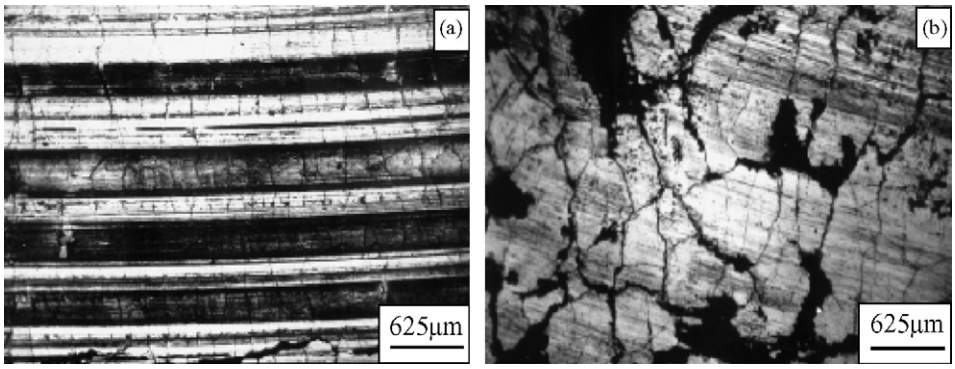

Fig. 7. Microstructure on friction surfaces of C/SiC disks.

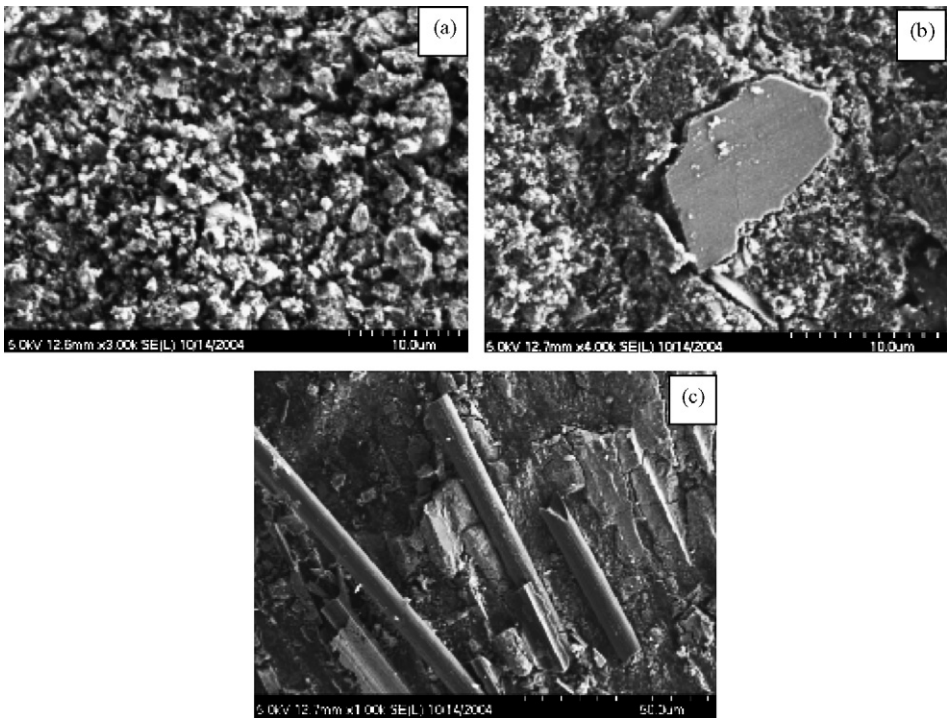

Fig. 8. SEM micrograph of the wear debris on the surfaces of C/SiC composites brake disk (a) worn grain covered on the surface, (b) a thin flake of material in the wear debris and (c) fragmentation of carbon fiber in wear debris on the surface.

increase with the increase of carbon content and material density from types A to D, while the values are in the same order of magnitude.

The surface microstructure and wear debris on wear-induced surfaces of C/SiC disks were investigated by an optical microscope and the SEM analysis. After the braking tests, the surfaces of C/SiC brake disks were covered with wear debris or grains (Fig. 8(a)) including the flake materials (Fig. 8(b)) and fragments of fiber (Fig. 8(c)). Tribological contact was mainly determined by solid–solid interactions between asperities on the mated surfaces of C/SiC disks. Depending on the initial roughness and the applied load, the grooves on the surfaces (Fig. 7(a)) along with the sliding direction, resulted from relative movement of large scale of adhesion conjunction or asperities. The mechanical and thermal stresses were continuous (constant load) between the contact asperities, which showed localized fatigue phenomena related to the displacement of wear areas (contact forces were not confined to the same asperities throughout the test). These cyclic fatigue phenomena made the material produce peeling and flakes (Fig. 8(b)). Under load and at the start of a test, before the temperature increase had affected the surface hardness, the abrasion was associated with a significant cracking [12]. Majority of the micro-cracks were radial cracking where the orientation was close to perpendicular to the movement (and to the direction of the abrasion grooves) (Fig. 7(a)). Moreover, the higher local temperature on the surfaces caused by serious

Table 2
The wear rate of C/SiC composite disks after the braking tests

Linear wear rate (μm/cycle)	A	B	C	D
Rotating disk	1.2	1.4	5.3	9.3
Stationary disk	1.0	0.9	–	2.5

relative sliding of hard material resulted in some lattice-like cracks named tortoiseshell cracks (Fig. 7(b)).

4. Conclusions

(1) The three-dimensional C/SiC (CVI) composites exhibited good mechanical properties, especially excellent shear strength. The damaged specimen showed non-brittle failure behavior resulted from the single fiber pull-out and fiber cluster pull-out. The in-plane shear strength and the inter-laminar shear strength were 85 and 27 MPa, respectively.
(2) The chemical vapor infiltration process offered a potential method to manufacture the C/SiC composites of high braking performance and wear resistance. With the material density of 2.3 g/cm^3, the average coefficient of friction was 0.23, the coefficient of friction stability remained about 0.43, and the wear rate was less than 9.3 μm/cycle.
(3) The C/SiC composites specially demonstrated a good stability of braking against fading versus several braking stops.
(4) The coefficient of friction and friction stability of C/SiC composites were significantly improved by increasing carbon content and material density. The rapid increase of friction coefficient when approaching the end of braking was mainly related to the rapid temperature increasing in a short time, the decreasing sliding velocity and the enhanced adhesion and abrasion of contact conjunctions or asperities.
(5) The surfaces of C/SiC brake disks were covered with wear debris including fragments of carbon fibers and flake materials after braking tests. The wear was significantly determined by cyclic mechanical and thermal stresses, which resulted in micro-cracks and grooves on friction surfaces.

Acknowledgements

The authors acknowledge the financial support of Natural Science Foundation of China (Contract No. 90405015), the Graduate Starting Seed Fund of Northwestern Polytechnical University (Contract No. Z200511) and the Natural Science Foundation of Shaanxi Province of China (Contract No. 2004E$_1$16).

References

[1] W. Krenkel, B. Heidenreich, R. Renz, C/C-SiC composites for advanced friction systems, Adv. Eng. Mater. 4 (2002) 427–436.
[2] E. Fitzer, The future of the carbon–carbon composites, Carbon 25 (1987) 163–190.
[3] T. Windhorst, G. Blount, Carbon–carbon composites; a summary of recent developments and applications [J], Mater. Des. 18 (1997) 11–15.
[4] S. Awathi, L. Wood, C/C composite material for aircraft [J], Adv. Ceram. Mater. 3 (1988) 449–451.
[5] W. Krenkel, Cost effective processing of composites by melt infiltration (LSI-Process), Ceram. Eng. Sci. Proc. 22 (2001) 442–444.
[6] R. Kochendorfer, Low cost processing for C/C-SiC composites by means of liquid silicon infiltration, Key Eng. Mat. 164–165 (1999) 451–456.
[7] Z.S. Pak, C$_f$/SiC/C composites for tribological application, Key Eng. Mat. 164–165 (1999) 820–825.
[8] J.-Y. Paris, L. Vincent, J. Denape, High-speed tribological behaviour of a carbon/silicon carbide composite, Com. Sci. Tech. 61 (2001) 417–423.
[9] S. Vaidyaraman, M. Purdy, T. Walker, S. Horst, C/SiC material evaluation for aircraft brake application, Key Eng. Mat. 164–165 (1999) 802–808.
[10] Y. Xu, L. Cheng, L. Zhang, Mechanical properties of 3D fiber reinforced C/SiC composites, Mater. Soc. Eng. A300 (2001) 196–202.
[11] S. Wen, Tribology Theory, Tsinghua University Book Concern, Beijing, 1991, pp. 398–470.
[12] K.-H. Zum Gahr, R. Blattner, D.-H. Hwang, K. Pohlann, Micro- and macro-tribological properties of SiC ceramics in sliding contact, Wear 250 (2001) 299–310.